Contrib Mineral Petrol (1999) 135: 212–224

A. Matthews · J. Lieberman · D. Avigad · Z. Garfunkel

Fluid-rock interaction and thermal evolution during thrusting of an Alpine metamorphic complex (Tinos island, Greece)

Received: 14 April 1998 / Accepted: 9 December 1998

Abstract This study examines the fluid-rock interaction and thermal evolution along a thrust that juxtaposes calcite-rich marbles of high P-T metamorphic unit of the Attic-Cycladic Massif (Greece) on top of a lower-grade dolomite marble unit. The Tertiary thrust represents a major phase of tectonic movement related to the decompression of the Alpine orogen in the Hellenides. The stable isotope signatures of the thrust plane and adjacent sections of the footwall and hanging wall rocks are characterized by significant carbon and oxygen isotope depletions. The depletion is most pronounced in calcite, but is almost entirely missing in coexisting dolomite. The isotopic patterns in the thrust zone can be explained by the infiltration of an externally derived water-rich H_2O-CO_2-CH_4 fluid [X_C $(=X_{CO_2}+X_{CH_4}) < 0.05$] at water-rock ratios on the order of 0.1 to 0.5 by weight. The fluid-induced calcite recrystallization is viewed as an important rheological control during thrusting. The temperature evolution of the footwall, hanging wall and mylonitic tectonic contact was determined by calcite-dolomite solvus thermometry. Histograms of calcite-dolomite temperatures are interpreted as indicating a heating of the footwall dolomite marble during the thrusting of the hotter upper plate. Conversely, the hanging wall marble unit was cooled during the thrusting. The calcite-dolomite thermometry of the thrust plane gives temperatures intermediate between the initial temperatures of the lower and upper marble units, and this leads to the conclusion that conductive heat transfer rather than fluid infiltration controlled the thermal evolution during thrusting.

A. Matthews (✉) · J. Lieberman · D. Avigad · Z. Garfunkel
Institute of Earth Sciences, Hebrew University of Jerusalem, 91904 Jerusalem, Israel

Editorial responsibility: J. Hoefs

Introduction

Studies of a tectonic contact in the area of Panormos Bay on the island of Tinos in the Attic-Cycladic Massif (ACM) of Greece (Fig. 1) address a current dilemma in the study of high pressure-low temperature (high P-T) metamorphism and orogeny. The P-T conditions of equilibrium for blueschists and eclogites generally lie at higher pressures and lower temperatures than most normal geothermal gradients. Thermal modelling suggests that only exceptionally rapid uplift will prevent re-establishment of an equilibrium geothermal gradient with consequent heating and destruction of the high P-T mineral assemblages (England and Thompson 1984; Thompson and Ridley 1987). Yet, abundant field, thermometric and age data from the ACM and elsewhere show that high P-T rocks were commonly uplifted and decompressed with little heating or even cooling (Matthews and Schliestedt 1984; Wijbrans et al. 1990; Avigad et al. 1992; Bröcker et al. 1993). Extensional tectonism has been suggested as an effective mechanism for crustal thinning and exhumation of orogen (e.g. Crittenden et al. 1980; Platt 1987, 1993; Avigad and Garfunkel 1991). Alternatively, underthrusting of the high P-T rocks by a package of cooler lower-grade rocks accompanied by erosion or tectonic denudation above the hanging wall would result in both decompression and absence of substantial heating during uplift.

The ACM is part of the Alpine orogen in the Hellenides, with a geological history dominated by Eocene blueschist to eclogite-facies metamorphism related to the Apulian-Eurasian plate collision. The exhumation of ACM has been assigned to the Oligo-Miocene low-angle back-arc extensional tectonism (Lister et al. 1984; Ridley 1984; Avigad and Garfunkel 1989, 1991; Buick 1991; Avigad 1993; Gautier et al. 1993; Lee and Lister 1992; Gautier and Brun 1994), although Avigad and Garfunkel (1995) and Avigad et al. (1997) pointed out that a considerable part of the decompression from high P-T conditions probably occurred prior to the onset of the

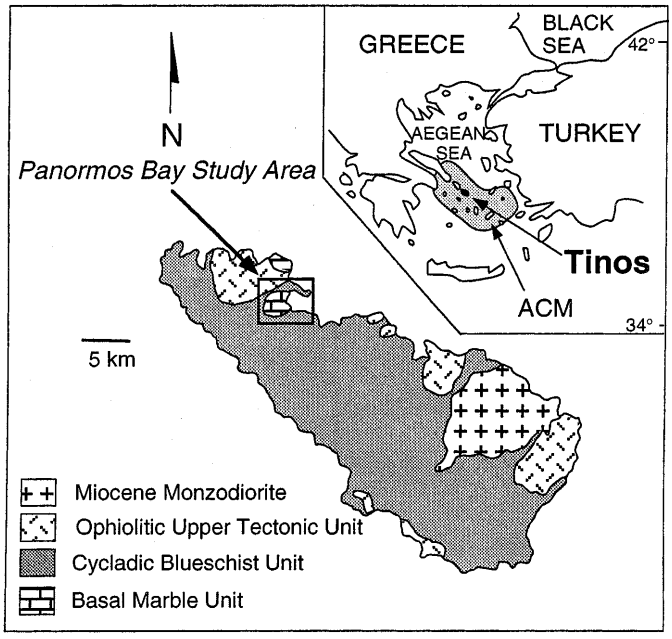

Fig. 1 Geological map of Tinos, showing the location of the Panormos Bay area. The *Basal Marble Unit* (M1 Marble of Melidonis 1980) consists of the Lower Dolomite marble and the Upper Marble discussed in the text. Overlying this is *Cycladic Blueschist Unit*, which in turn is tectonically overlain by the *Ophiolitic Upper Tectonic Unit*. The *Miocene Monzodiorite* intrudes both the Blueschist Unit and the Upper Tectonic Unit. Map modified after Melidonis (1980)

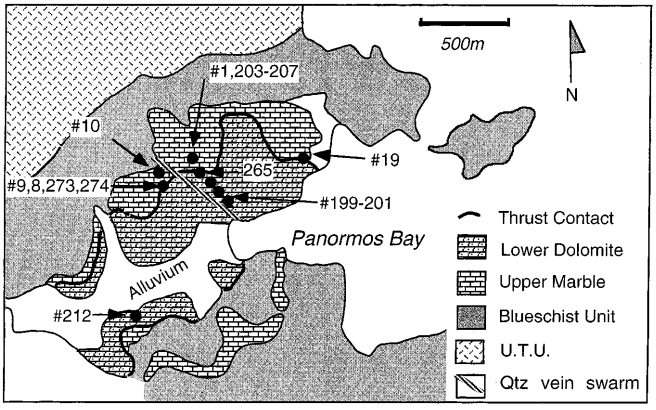

Fig. 2 Geological sketch map of the Panormos bay area (after Avigad and Garfunkel 1989) with sample location sites in study. *U.T.U.* signifies the Upper Tectonic Unit

tectonism. A characteristic feature of the interval between the peak of high P-T metamorphism and the commencement of back-arc extension was the development of thrust faults that emplaced partially exhumed high P-T rocks over lower grade metamorphic units (Avigad et al. 1997). One such thrust fault was identified in the Panormos Bay area of NE Tinos. The tectonic contact occurs within a marble unit that had formerly been considered, part of the high P-T blueschist sequence. However, in the Panormos Bay exposures (Fig. 2), calcite marble (Upper Marble) containing relict high P-T minerals overlies a dolomite marble (Lower Dolomite) in which equivalent metamorphic relics have not been found, and in which the preservation of fossil remnants suggests absence of extensive metamorphism. The evidence for structural discordance and discontinuity in the metamorphic grade (i.e. higher grade rocks over lower units) led Avigad and Garfunkel (1989) to propose that a thrust fault had transposed high P-T rocks over a cooler higher-level unit. Thrust faults of the type observed at Panormos Bay have also been identified elsewhere in the ACM – on the island of Euboia. They are also known in other Mediterranean back-arc basins (e.g. the Alboran and Tyrrenian Seas) developed in sites previously thickened by Alpine orogenesis (cf. Avigad et al. 1997).

The aim of this study was to examine the fluid-rock interaction and thermal evolution during thrusting in the Panormos Bay. This objective was achieved by determination of the microstructural, stable-isotope and thermometric differences between the foot- and hanging-walls of the Panormos Bay tectonic contact.

The stable isotope studies addressed the fluid-rock interaction. Numerous studies have investigated the relationship between fluids and deformation, since the pioneering work of Hubbert and Rube (1959) showed that thrusting requires fluid pressures close to, or even higher than, lithostatic pressures. Stable isotope fractionations are powerful tracers of fluid-rock interaction and over the last two decades have provided substantial evidence for fluid infiltration along shear- and fracture-zones (e.g. Beach and Fyfe 1972; Kerrich et al. 1984; Burkhard and Kerrich 1988; McCaig 1988; Rye and Bradbury 1988; Fourcade et al. 1989; McCaig et al. 1990, 1995; Burkhard et al. 1992; Fricke et al. 1992; Cartwright et al. 1993; Oliver et al. 1993; Morrison 1994; Peters and Wickham 1994; Crespo-Blanc et al. 1995; Eppel and Abart 1997; Morrison and Lawford Anderson 1998). The present study shows that fluid infiltration plays a critical role in the rheology of a thrust system, although the thermal regime was controlled by conductive heat transport.

Geological background

The Cycladic metamorphic complex is an Alpine terrane formed by the Tertiary collision of the Apulian microplate with the Eurasian plate. Subduction to depths of 50 km or more led to the development of Eocene high P-T metamorphic assemblages. Maximum metamorphic conditions have been estimated at 500 °C and 16 kbar (Matthews and Schliestedt 1984; Schliestedt 1986; Schliestedt et al. 1987; Okrusch and Bröcker 1990). The high P-T metamorphism was followed by a regional Oligocene–Miocene overprint during decompression. In the western Cyclades, where the island of Tinos is situated, the overprint is reflected by the development of a greenschist fabric at P-T conditions of ca 450–500 °C and 5–8 kbar (Matthews and Schliestedt 1984; Schliestedt et al. 1987; Schliestedt and Matthews 1987; Avigad et al. 1992; Bröcker et al. 1993; Schliestedt et al. 1994). The regional metamorphic overprinting was succeeded by a Miocene intrusion of granitoid magmas (Altherr et al. 1982, 1988). The high P-T sequences (Cycladic Blueschist Unit), are structurally overlain by the Upper Tectonic Unit (Durr et al. 1978) which comprises a variety of lithologies that did not

experience high pressure metamorphism. The tectonic contacts of the two units are shallow-dipping normal faults (Lister et al. 1984; Ridley 1984; Avigad and Garfunkel 1989, 1991).

Tinos was first mapped in detail by Melidonis (1980) (Fig. 1). The Blueschist Unit dominates the geology of the island, where high P-T metamorphism has been dated at 40–44 Ma and the subsequent greenschist overprint at 21–23 Ma (Bröcker et al. 1993). The greenschist fabric is particularly marked in the structurally lower parts of the Blueschist Unit, where the Panormos Bay marble outcrops. The Blueschist Unit rocks and late Cretaceous metamorphosed ophiolites that belong to the Upper Tectonic Unit (Avigad and Garfunkel 1989; Katzir et al. 1996; Stolz et al. 1997) are intruded by a Miocene (ca 18 Ma, Altherr et al. 1982; 1988) monzodiorite. The low angle tectonic contact that juxtaposes the ophiolitic Upper Tectonic Unit onto the Blueschist unit was possibly syn-orogenic (Avigad et al. 1997).

Geology of the Panormos Bay Marbles

The Panormos Bay Marble sequence is exposed in the core of an upright antiform (Fig. 2). The base of the section consists of the more than 100-m thick buff-coloured Lower Dolomite unit containing Upper Triassic fossils (algae, coral fragments, and echinoids), which preserve their original shape and fabric (Melidonis 1980; Avigad and Garfunkel 1989). The dolomites are discontinuously overlain by a 1–2-m thick horizon of mylonitic quartzites interleaved with micaceous phyllites (Fig. 3). The phyllites have schistosity defined by preferred orientation of micas in a sub-polygonal quartzo-feldspathic matrix. The dolomite unit is overlain by the Blueschist Unit that comprises at its bottom an approximately 50-m thick well-layered grey-coloured Upper Marble sequence, also overlain by metasedimentary and metavolcanic schists. On the southern flank of the antiform, a tectonic contact is truncated and the schists often directly overlie the Lower Dolomite (Fig. 2). The Blueschist Unit schists in the Panormos Bay area were strongly overprinted by retrograde greenschist-facies metamorphism.

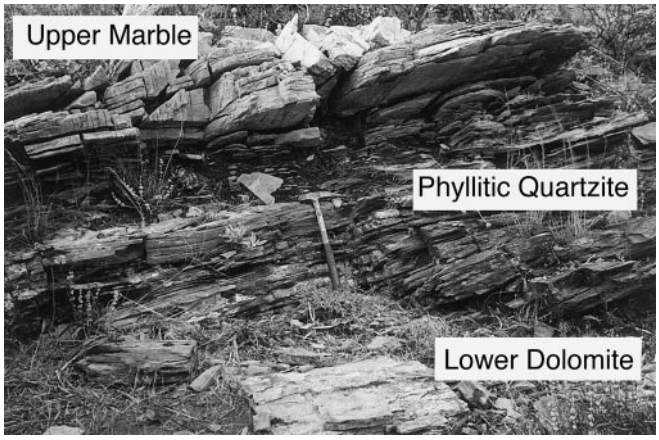

Fig. 3 Photograph of the mylonitic tectonic contact showing the *Upper Marble* (grey coloured) overlying the phyllitic quartzite. The *Lower Dolomite* (buff coloured) can be seen at the bottom of the photograph

Samples for this study were taken from the foot- and hanging-wall of the marbles and the mylonitic tectonic contact. The main sample locations are given in Fig. 2 and Table 1 is a summary of the locations, mineralogy and main petrographical characteristics of individual samples. Relevant features of the mineralogy and microstructures of the three principal lithological units are briefly described below.

Lower Dolomite (Lower Plate)

This varies from calcite-absent dolomites to dolomite-rich marbles containing small amounts of calcite, quartz, and mica. Two generations of carbonate were observed in thin section: relict dolomite and calcite porphyroclasts surrounded by finer recrystallized grains.

Table 1 Sample location sites and descriptions. (*L. dolomite* (*L. dol*) Lower Dolomite, *U. marble* (*U. mb*) Upper Marble. *rxt* recrystallized, *cc* calcite, *dol* dolomite)

Sample location no.	Unit	Approx. vertical distance from contact (m)	Textural characteristics of samples
199	L. dolomite	−90	rxt cc & dol/relict dol clasts
200	L. dolomite	−50	rxt cc & dol/relict dol clasts
212	L. dolomite	−40	rxt cc & dol/relict dol clasts
201	L. dolomite	−30	rxt cc & dol/relict dol clasts
265	L. dolomite	−2	fine-grained rxt cc & dol/relict dol clasts
274	L. dolomite	−1	fine-grained rxt cc & dol/rare dol clasts
273	Mylonitic contact (L.dol)	< -0.5	Strained highly rxt cc & dol/no clasts
9.3	Mylonitic contact (L.dol)	< -0.5	Strained highly rxt cc & dol/no clasts
9.1	Mylonitic quartzite	0	rxt phyllitic quartzite/N-trending folds
9.4	Mylonitic contact (U.mb)	< 0.5	Strained highly rxt cc & dol
8	U. marble	+5	rxt cc & dol/abundant relict cc & dol clasts
203a	U. marble	+20	rxt cc & dol/abundant relict cc & dol clasts
203b	U. marble	+20	cc segregation from 203a
206	U. marble	+20	Quartzitic marble with neoformed cc
10.3	U. marble	+20	rxt cc & dol interlaminated with cc & dol clasts
10.4	U. marble	+20	quartzitic marble with neoformed cc
1	U. marble	+25	rxt cc & dol interlaminated with cc & dol clasts
205	U. marble	+25	rxt cc & dol interlaminated with cc & dol clasts
207	U. marble	+25	rxt cc & dol interlaminated with cc & dol clasts
19.1	U. marble	+5–10	rxt cc/abundant relict cc clasts
19.2	U. marble	+5–10	rxt cc/abundant relict cc clasts
19.3	U. marble	+5–10	rxt cc/abundant relict cc clasts

Tectonic Contact Mylonite

Samples were mainly taken from a site where the mylonitic quartzite at the contact zone is particularly well exposed (Fig. 3). The samples (#9, 272, 273) from this locality comprise the mylonitic quartzite, the Lower Dolomite and Upper Marble that occur immediately above and below the quartzite respectively (Fig. 3; Table 1). The marble is mylonitic fine-grained, recrystallized and lacks relics of calcite and dolomite porphyroclasts. The quartzite consists of fine-grained, highly strained, recrystallized quartz with N-trending microfolds interleaved with centimetre-thick mica-rich bands.

Upper Marble (Upper Plate)

The Upper Marble is a calcite-rich marble containing varying amounts of dolomite, with thin bands of quartzite, schistose lenses containing typical Eocene high P-T metamorphic minerals (garnet, epidote) and Oligo-Miocene greenschist overprint (albite & chlorite). This marble shows a coarse polygonal unstrained texture characteristic of other marbles in the Cycladic Blueschist Unit. This coexistence of relict porphyroclasts and a surrounding matrix of finer recrystallized grains sometimes takes the form of a laminated texture where varying amounts of fine grained quartz and recrystallized calcite are interleaved with coarser carbonate minerals (cf. #Ti-1; 205; 10.3). Two samples (#206; 10.4) are impure quartzites with calcite and dolomite in which the calcite conspicuously occurs as a neo-formed infilling showing no evidence of strain.

The rock fabrics described above indicate that the original textures (represented by dolomite clasts in the Lower Dolomite and calcite and dolomite clasts in the Upper Marble) were overprinted during the deformation that increased in intensity towards the tectonic contact. This suggests that the deformation and recrystallization were related to the thrusting event that juxtaposed the Blueschist Unit onto the Lower Dolomite. The presence of neo-formed strain-free recrystallized grains also suggests that deformation and recovery continued after movement on the thrust plane ceased. In addition to the texture of the marble, the rock sequence is cut by a steeply inclined quartz vein system (Fig. 2) and the tectonic contact displaced approximately 20 m vertically on either side of this vein system, suggesting that vein fluids infiltrated along a late normal fault. In order to understand the origin of this quartz vein system, samples of quartz were taken along its length for oxygen isotope study.

Methods

All samples were examined in thin section and staining with acidified Alizarin S was used to differentiate between dolomite and calcite. The carbonate mineralogy was checked by X-ray powder diffraction. Carbon and oxygen isotopes were analysed using conventional 25 °C phosphoric acid methods (McCrea 1950). Dolomite extractions were made on pure separates prepared by dissolving coexisting calcite with dilute acetic acid. The separates were treated with phosphoric acid for 7 days at 25 °C. Calcite extractions from pure calcite samples were obtained by treatment with phosphoric acid for 24 h, and from mixed dolomite-calcite samples by varying the time from ca. 15 min to 1 h. The oxygen for silicate analyses was extracted using the bromine penta-fluoride procedure of Clayton and Mayeda (1963). A number of the silicate analyses were made using the laser fluorination extraction system at the Hebrew University. A Merchantek EO MIR laser ablation station, BrF_5 reagent and a VG Micromass 602 ES Mass Spectrometer were used in the system. Based on the analyses of standards, $\delta^{18}O$ values are accurate to $\pm 0.2‰$, except for the short-time calcite extractions, where accuracy is $\pm 0.3‰$. Carbon isotope analyses are accurate to $\pm 0.15‰$.

Temperatures were determined by dolomite-calcite solvus thermometry (Goldsmith and Newton 1969; Essene 1985). The choice of the dolomite-calcite solvus thermometry methodology was influenced by the fact that the temperature range being investigated is below that at which Mg/Ca exchange occurs in a dolomite-calcite system. This system is generally considered to show diffusional closure at ca. 500–600 °C (Essene 1985; Lieberman and Rice 1986). The samples studied in this work show evidence of recrystallization, which can allow cation equilibration to occur at temperatures lower than those of diffusional closure. To present as complete a picture as possible of the temperatures of cation equilibration, a large number of EPMA spot analyses were made on samples taken from both sides of the tectonic contact, as well as from the contact. The analyses were made by electron microprobe using a Tracor System II automated Jeol 8600 instrument at beam conditions, 15 kV and size 5–25 microns.

Carbon and oxygen analyses for marbles and dolomite-calcite thermometry results are presented in Figs. 4–6. (Tables of carbonate isotopic data and microprobe analyses may be obtained in writing from the authors).

Results

Carbon and oxygen isotope compositions

The oxygen isotope results for dolomites and calcite are plotted in Fig. 4 as a function of their relative vertical heights in the Panormos Bay sequence. The heights in Fig. 4 and Table 1 are with reference to the tectonic contact, arbitrarily assigned a value of zero. The vertical band in the diagram gives the range of $\delta^{18}O$ values typically observed for dolomites and calcites from marbles in the Cyclades (Rye et al. 1976; Matthews and Schliestedt 1984; Baker et al. 1989; Ganor et al. 1989, 1991, 1994; Baker and Matthews 1994, 1995). The high $\delta^{18}O$ values for these marbles reflect a marine sedimentary protolith. The dolomites analysed in this study plot within the metamorphic marble range. These are; *Lower Dolomite* ($\delta^{18}O$ 28–31‰), *Upper Marble* (29.5–31.5‰),

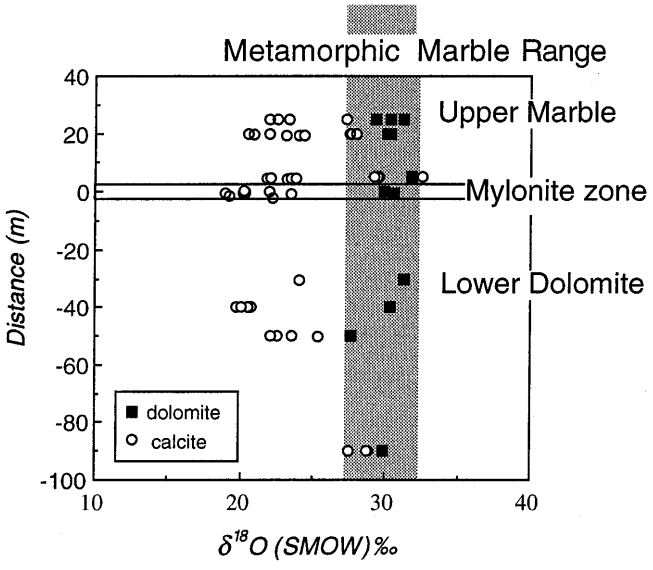

Fig. 4 A plot of the $\delta^{18}O$ values for calcites and dolomites vs vertical distance in the section (zero is arbitrarily set at the middle of the tectonic contact). The definition of the *Metamorphic Marble Range* is given in the text

and dolomite from the mylonitic tectonic contact (~30‰). If coexisting calcites were in isotopic equilibrium with the dolomites, we would anticipate their $\delta^{18}O$ values to be 27–31‰ (based on the dolomite-calcite fractionation of Matthews and Katz, 1977). However, a very few values plot in this range and the calcite analyses instead seem to show a broad trend of decreasing $\delta^{18}O$, with the lowest values ~20‰ occurring in the calcite samples from the tectonic contact. This $\delta^{18}O$ range is unique to the marbles in the Cyclades. It is thus clear that some processes have influenced the oxygen isotope composition of the calcites, but not those of the dolomites, and that these processes are focused about the tectonic contact. The few calcites showing $\delta^{18}O$ values of the metamorphic marble range are from the Upper Marble samples (e.g. #8) with *significant amounts* of relict porphyroclasts and a Lower Dolomite sample (#199) 90 m below the contact. The most likely process for the decrease of the $\delta^{18}O$ values is isotope exchange accompanying the infiltration of low $\delta^{18}O$ fluids.

Figure 5 is a $\delta^{13}C$ *vs* $\delta^{18}O$ plot for dolomites and calcites of the Panormos Bay sequences. Dolomite $\delta^{13}C$ values are ca. 2–3‰, again in the range typical of metamorphic marbles in the Cyclades. A significant number of calcite samples have $\delta^{13}C$ values 1–2‰, but as $\delta^{18}O$ values of calcite drop below 22‰ there is a clear trend of decreasing $\delta^{13}C$, with the lowest values to −6‰ in samples from the mylonitic tectonic contact. As a whole, the data define a curvilinear array for $\delta^{13}C$ and $\delta^{18}O$. The Upper Marble and Lower Dolomite calcites largely define a trend of decreasing $\delta^{18}O$ at typical metamorphic $\delta^{13}C$, whereas samples from the contact zone strongly show sharply decreasing $\delta^{13}C$ for $\delta^{18}O < 22$‰. The data array exhibited in Fig. 5 is similar to that of model curves (e.g., Rye and Bradbury 1988; McCaig et al. 1995) generated for infiltration of an ^{18}O- and ^{13}C-depleted fluid into a pre-existing metamorphic marble. The mylonite zone calcite samples represent rocks mostly influenced by the infiltrating fluid and it is important to note that the isotopic depletion (Fig. 4) is only observed in the calcite samples. Dolomite samples show little or no changes in isotopic compositions and probably represent unaltered marbles that have not been affected by fluid-rock exchange.

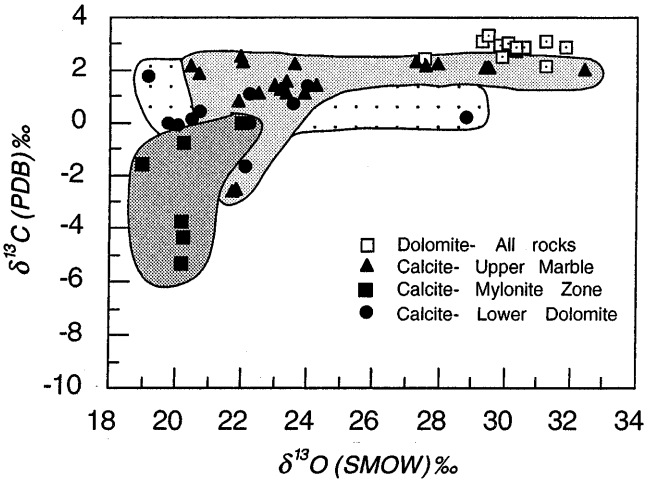

Fig. 5 $\delta^{13}C$ vs $\delta^{18}O$ plot for calcite and dolomite. Dolomites are grouped together, whereas calcites are grouped according to the rock-type from which they are sampled

Oxygen isotope analyses for quartz samples are given in Table 2. The quartz separates from the marbles show distinct differences. Three separates from the Upper Marble give $\delta^{18}O$ values of ca. 31‰. Dolomite – quartz equilibrium fractionations are very small at metamor-

Table 2 Oxygen isotope analyses of silicates and coexisting carbonates

Sample no.	Location	Sample	$\delta^{18}O$ (SMOW) ‰
AM91-Ti-9.1	Mylonite zone (Phyllitic quartzite) (0 m)	Quartz Whole-rock	28.4 23.3*
AM93-Ti-272	Mylonite zone (phyllitic quartzite) (0 m)	Quartz	28.7
J191-Ti-9.3	Mylonite zone (L. Dolomite) (< −0.5 m)	Quartz Dolomite Calcite	25.1 ± 0.2* 30.6 20.3
AM93-Ti-267	Quartzite segregation (Upper Marble +4 m)	Quartz	31.0
J191-Ti-1	Upper Marble (+25 m)	Quartz Dolomite Calcite	31.1 ± 0.2* 30.3 23.0
AM91-Ti-205	Upper Marble (+25 m)	Quartz Dolomite Calcite	31.4 ± 0.1* 31.2 27.3
Late quartz veins			
AM93-Ti-261	Lower Dolomite (−90 m)	Quartz	6.4
AM93-Ti-264	Lower Dolomite (−40 m)	Quartz	4.9
AM93-Ti-268	Upper Marble (+40 m)	Quartz	8.6

* Laser fluorination analysis

phic temperatures and the quartz $\delta^{18}O$ values are in the range anticipated for isotopic equilibrium with dolomite. This means that neither dolomite nor quartz have undergone isotopic exchange with the infiltrating fluid that lowered $\delta^{18}O$ in the calcite. In contrast, a $\delta^{18}O$ value of 25.1‰ was determined for quartz in a Lower Dolomite marble of the mylonitic contact zone (#9-3). This is significantly lower than the $\delta^{18}O$ value (30.6‰) for the dolomite in this rock and suggests that the quartz has undergone isotopic exchange with the infiltrating fluid. The high $\delta^{18}O$ values (~28.5‰) for two mylonitic quartzite samples clearly show that the precursors for rocks were cherts rather than sandstones. Jurassic to Cretaceous marine cherts have $\delta^{18}O$ values >31‰. (Kolodny and Epstein 1976), which may suggest that there has been exchange with the infiltrating fluid. A micaceous phyllite layer within the quartzite gives a whole rock $\delta^{18}O$ value of 23.3‰.

The above quartz $\delta^{18}O$ values contrast remarkably with those (5–8‰) obtained from the quartz vein system. The contrasting $\delta^{18}O$ values clearly indicate a totally different fluid for the vein system from that involved in the fluid infiltration of the marbles. The fluid for the vein must have developed at relatively low temperatures and from water with a negative oxygen isotopic composition. For example, at 200 °C the quartz-water fractionation is approximately 12‰ (Matsuhisa et al. 1979; Matthews and Beckinsale 1979) and the calculated fluid composition is −7 to −4‰. These are within the general range of $\delta^{18}O$ values (−8 to −4‰ Rozanski et al. 1993; Gat 1996) for present day meteoric water in the Mediterranean and southern European region. Lower temperatures for the vein formation would give more negative water isotopic compositions. It is thus clear that the quartz veins formed from downward percolation of groundwater and have no connection with the fluid that infiltrated the tectonic contact.

Dolomite-calcite solvus thermometry

The dolomite-calcite solvus thermometry results are presented as a series of histograms (Fig. 6a–c). Temperatures were calculated using the equation of Lieberman and Rice (1986). Temperature histograms for the Lower dolomite are given in Fig. 6a. The three samples show a spread of temperatures from ca. 200 °C with maxima between 300 °C and 400 °C. The temperatures at which these peak distributions occur are apparently correlable with distances from the contact: ca. 300 °C for #199 (−90 m); 340 °C for #200 (−50 m): 370 °C for #212 (−40 m).

The two samples analyzed for the mylonitic contact zone were taken from the Lower Dolomite (#9.3) and Upper Marble (#9.4) that lie immediately below and above the mylonitic quartzite, respectively. A striking feature of the results (Fig. 6b) is the apparent bimodal distribution of temperatures, particularly evident in Upper Marble sample (#9.4) where a large number (150) of analyses were made. The modes of the distributions are at approximately 280–320 °C and 370–420 °C in both samples, with peaks at ca. 300 °C and 400 °C, respectively. The distributions of temperature in both samples differ from those given in Fig. 6a (Lower Dolomite) and Fig. 6c (Upper Marble). The Upper Marble samples show more complicated distributions (Fig. 6c), with four of the samples having temperature distribution peaks at approximately 360–420 °C. These include samples (#203a; 205) that show a relatively narrow spread of temperatures and (#1; 10.3) that show skewed distributions with tailing towards lower temperatures of 300 °C or less. Samples # 10.4 and 206 show markedly lower temperature distributions with peaks ~300–320 °C. These latter two samples are located at approximately the same distance from the contact as the samples showing the higher temperature distributions. This therefore implies that there is no obvious relationship between temperature and proximity to the contact for the Upper Marble. This observation, however, contrasts with the trend in the microstructures of the samples. Whereas the four samples showing higher temperature distributions contain both relict porphyroclasts and strained recrystallized carbonate, the two that show lower temperatures contain only unstrained neoformed carbonate (Table 1).

Discussion

Fluid infiltration

The stable isotope results of this study are consonant with those of previous works (e.g. Beach and Fyfe 1972; Burkhard and Kerrich 1988; Rye and Bradbury 1988; Burkhard et al. 1992; McCaig et al. 1995) indicating that externally derived fluids syntectonically infiltrate ductile shear zones. The fact that isotopic shifts are found in rocks of both the foot- and hanging-walls, as well as in the mylonitic rocks, indicates that fluid mobilization was not restricted to the mylonite zone, but occurred over a heterogeneous infiltration zone (Fig. 4) up to 100 m wide. Nonetheless, fluid flow was dominantly focused along the tectonic contact.

The $\delta^{13}C$ vs. $\delta^{18}O$ plot (Fig. 5), suggests that the calcite in equilibrium with the infiltrating fluid has a $\delta^{18}O$ value of ca. 19–20‰. At 400 °C the $\delta^{18}O$ of the water in equilibrium with this calcite would be ~15.5–16.5‰ (cf. calcite-water fractionation of O'Neil et al. 1969). These values are not in the range for fluid in oxygen isotope equilibrium with any of the marble sequences nor represent groundwaters but potentially are in the range for waters in equilibrium with silicate lithologies. The low $\delta^{13}C$ value inferred for the fluid indicates an organic carbon source. The marble sequences of Tinos have a marine ^{13}C signature (Ganor et al. 1994) and carbonate sequences that could produce isotopically light decarbonation CO_2 are not found. Consequently,

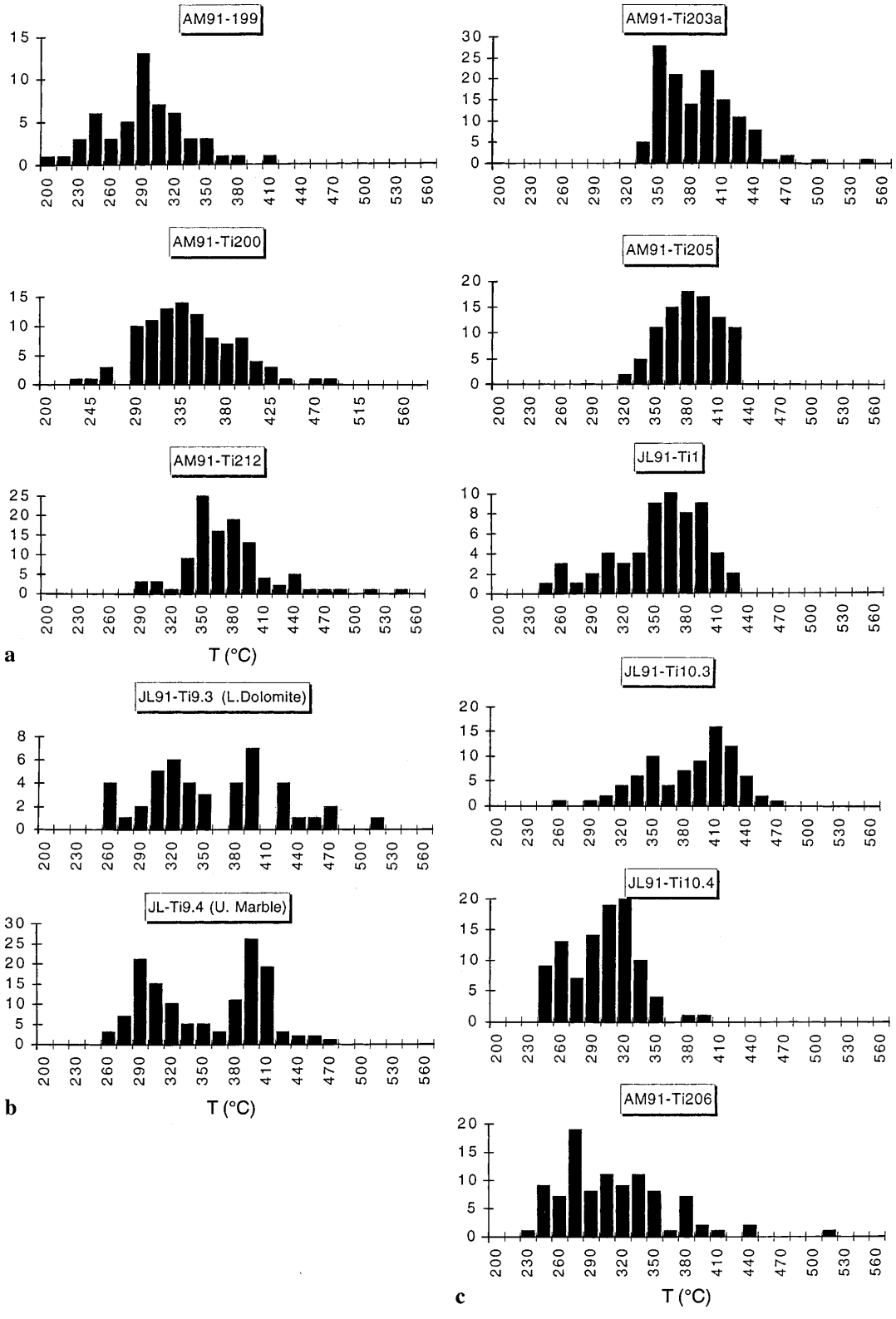

Fig. 6a–c Temperature histograms of the results of the Dolomite-calcite Mg-solvus thermometry calculated using the calibration of Lieberman and Rice (1986). (6a = *Lower Dolomite* results; 6b = *mylonitic tectonic contact* results; 6c = *Upper Marble* results)

the most likely origin of ^{13}C-depleted carbon is the oxidation of carbonaceous matter.

The oxygen isotopic composition of the fluid does not favour a long range transport of fluids from the surface (e.g. meteoric or sea water) and magmatic fluids are not indicated. It suggests instead that the fluids were derived

from sources within the vicinity of the thrust zone (e.g. Grant et al. 1990; Banks et al. 1991). A possible mechanism for generating fluid movement is dilatancy-pumping (Sibson et al. 1975) which would have served to draw fluids from the foot- and hanging-walls into the mylonitized shear zone (e.g. Beach 1976; Etheridge et al. 1984: Reynolds and Lister 1987). Alternatively, the fluid may have been expelled from the lower plate as a result of overpressuring (Hubbert and Rubey 1959).

Within the exposures of Panormos Bay and its vicinity there are two potential sources for fluids:

(1) Water equilibrated with greenschist-facies rocks the Blueschist Unit (Fig. 2). We have noted that the Blueschist Unit rocks in the Panormos Bay area are strongly overprinted by a retrograde greenschist-facies event. $\delta^{18}O$ values for quartz from the greenschist-facies repeated rocks average ca. 16.5‰ (Bröcker et al. 1993). The water in isotopic equilibrium with these rocks would have $\delta^{18}O$ values ca. 14–15‰, which is reasonably close to the value (15.5–16.5‰) suggested above, especially if there was a small amount of exchange with the marbles. Movement of this water through the Upper Marble with oxidation of graphitic matter could thus provide an infiltration fluid with the required isotopic characteristics. There are no carbon isotope analyses of graphite on Tinos, but the data of Kreulen (1988) on Naxos give $\delta^{13}C$ (from graphite) values that mostly fall around −24 to −27‰. The greenschist overprint of the high-pressure metamorphic assemblages involves hydration and infiltration of a water-rich fluid (Schliestedt and Matthews 1987; Bröcker 1990). It is possible that the thrusting was contemporaneous with this overprint and involved the same fluid.

(2) Micaceous phyllite fluids. Devolatization of the micas of the micaceous phyllite in the repeat contact zone during the emplacement of the hotter upper plate, concomitant with the oxidation of graphite provides a viable alternative source of the infiltrating fluid. However, the $\delta^{18}O$ value (23.3‰, Table 1) of this micaceous phyllite is too high for a fluid with suitable oxygen isotope characteristics. The micaceous phyllite fluids source is therefore rejected in favour of fluids in equilibrium with greenschist-facies rocks.

Model of fluid-interaction

The quantification of fluid-rock interaction by one-dimensional transport equation modeling of isotopic profiles across lithological contacts (Bickle and McKenzie 1987; Baumgartner and Rumble 1988; Bickle and Baker 1990: Baker and Spiegelman 1995; Abart and Eppart 1997) is considerably advanced. Such inverse modeling, requires an appropriate data array in the form of an advective-dispersive front or a diffusional exchange profile centered at a lithological contact. Although the data array presented in Fig. 4 broadly define an infiltration zone, the fluid-rock interaction is heterogeneous at a local scale and the data do not define a one-dimensional front. Our modeling of the fluid-rock interaction therefore focuses on 'zero-dimensional' mass balance calculations, based on the equations of Taylor (1977) and Rye and Bradbury (1988).

The preceding discussion has suggested that the oxygen isotope composition of the infiltrating fluid is largely governed by equilibrium with the silicate rocks of the Blueschist Unit. The rocks of the Blueschist Unit are calcite-bearing (Bröcker 1990; Ganor et al. 1996) and thus it is likely that the fluid in equilibrium with them was quite close to saturation with calcite. This may account for the apparently very small contribution from the Upper Marble to the oxygen isotope composition of the fluid. It is assumed that the fluid was undersaturated with respect to graphite in the marble and that the dissolution of graphite gave rise to the isotopically light carbon in the fluid. In the absence of any other oxygen fugacity-buffering reaction, this mechanism would give rise to a *GCOH* fluid with an H/O ratio of 2:1. Calculations of equilibria in this system by Connolly and Cesare (1993) shows that $X_{CO_2} \cong X_{CH_4} \leq 0.02$ at 400 °C (other species can be neglected). The assumption that $X_{CO_2} = X_{CH_4}$ will therefore be carried forward into the isotopic calculations. Appropriate mass balance equations for C-O isotope covariation in calcite infiltrated by an H_2O-CO_2-CH_4 fluid with $X_{CO_2} = X_{CH_4}$ are:

$$\delta^{18}O^{f}_{CC} = \frac{(W/R)/3 \cdot (\delta^{18}O^{i}_{fl} + \Delta_o) + \delta^{18}O^{i}_{CC}}{(1 + (W/R)/3)}$$

$$\delta^{13}C^{f}_{CC} = \frac{(W/R)X_C \cdot (\delta^{13}C^{i}_{fl} + \Delta_C) + \delta^{13}C^{i}_{CC}}{(1 + (W/R)/X_C)}$$

where (W/R) is the closed system (CS) fluid/calcite ratio expressed in moles and is related to the single pass open system (OS) (W/R) ratio by the equation:

$$(W/R)_{OS} = \ln((W/R)_{CS} + 1) \text{ (Taylor 1977)}$$

$X_C (= X_{CO_2} + X_{CH_4})$ is the mole fraction of carbon in the H_2O-CO_2-CH_4 fluid phase, the superscripts i and f refer to the initial and final (after exchange) isotopic compositions and the subscripts *CC* and *fl* refer to the calcite and fluid phases respectively. Δ_o and Δ_C are the fractionations between calcite and fluid for oxygen and carbon respectively, and expressed by the equations:

$$\Delta_o = 1000 \ln \alpha_{CC-H_2O} \cdot (1 - X_C) + 1000 \ln \alpha_{CC-CO_2} \cdot X_C$$

$$\Delta_C = 0.5 \cdot 1000 \ln \alpha_{CC-CO_2} + 0.5 \cdot 1000 \ln \alpha_{CC-CH_4}$$

The calculation is made assuming the $\delta^{18}O$ of the H_2O-CO_2-CH_4 fluid ($\delta^{18}O^{i}_{fl}$) is constant (i.e. water provides all the oxygen in the system). Parameters assumed in the calculation are: $\delta^{18}O^{i}_{fl} = 16‰; \delta^{13}C^{i}_{fl} = -25‰; \delta^{13}C^{i}_{CC} = 2.5‰; \delta^{18}O^{i}_{CC} = 30‰$; T = 400 °C. Fractionation factors are taken from O'Neil et al. (1969) (*CC-H_2O*), Chacko et al. (1991) (*CC-CO_2*) and Bottinga (1969)(*CC-CH_4*). On a $\delta^{13}C$ vs. $\delta^{18}O$ plot, the mass balance equations define a series of curves with shapes dependent on X_C. The results of the calculation are plotted in Fig. 7 and show that almost all the Panormos Bay data correspond to a fluid with $X_C < 0.05$. The mass-balance calculations thus indicate that a water-rich

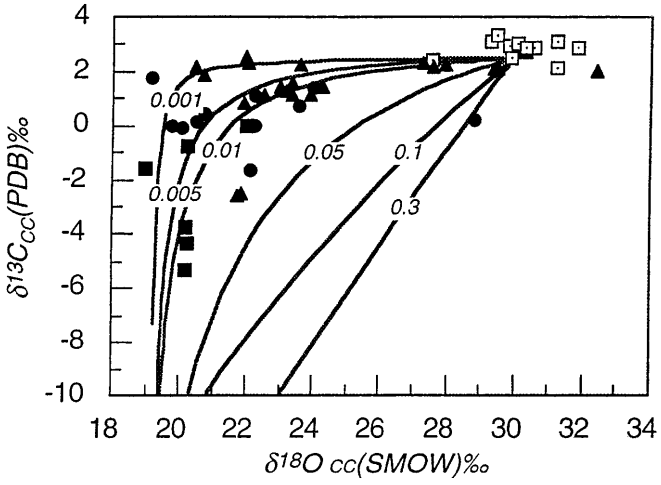

Fig. 7 Model fits for the infiltration of an H_2O-CO_2-CH_4 ($X_{CO_2} = X_{CH_4}$) fluid into the Panormos Bay marble units. Numbered isopleths represent values of Xc ($X_{CO_2} = X_{CH_4}$) in the fluid phase. The isotopic data plotted in the diagram are from Figure 5. Equations and parameters used in the calculations for the model are given in the text. The model shows a low Xc (≤0.05) fluid.

metamorphic fluid infiltrated the Panormos Bay exposure. The limits placed on X_C by the isotopic calculation are in excellent agreement with the speciation at 400 °C noted by Connolly and Cesare (1993) for a *GCOH* fluid with $H/O = 2$. Integrated fluid fluxes, expressed as minimum W/R weight ratios, vary from 0.1–0.5 at the contact, but decrease to < 0.1 further from the contact.

Isotopic exchange behaviour of minerals

A notable aspect of the results is the difference in the isotopic behaviour of calcite, quartz and dolomite. Whereas calcite has undergone isotopic exchange with the infiltrating aqueous fluid, quartz and dolomite have clearly not responded so readily to this fluid. The modeling of the carbon and oxygen isotopic variations for the calcite in this work has assumed that local-scale isotopic equilibrium is established between the mineral and fluid. The number of studies (e.g. Ganor et al. 1989; Bickle and Baker 1990; Eppel and Abart 1997) that have successfully modeled fluid-calcite exchange using the local equilibrium assumption justifies this premise. For quartz, however, a departure from the local equilibrium is observed (Eppel and Abart 1977). This raises the possibility that the differences in isotopic composition observed in calcite, quartz and dolomite at Panormos Bay reflect kinetically-controlled exchange of the latter two minerals.

Quartz in less-deformed rocks of the Upper Marble with a $\delta^{18}O$ value of ~31‰, similar to that of dolomite, has not undergone oxygen isotope exchange with the infiltrating fluid. The quartz is compared with calcite in the same samples, which shows lower isotopic compositions indicative of fluid-rock exchange (Table 2). In a strongly recrystallized Lower Dolomite marble at the mylonite tectonic contact (#9-3), quartz has an $\delta^{18}O$ value of 25.3‰, evidently indicative of isotopic exchange. However, the oxygen isotope fractionation (5‰) between quartz and calcite in this sample is too large for isotopic equilibrium, and indicates that the quartz has not fully equilibrated with the fluid. The mylonitic quartzite of the tectonic contact also shows slight lowering of $\delta^{18}O$ due to fluid-rock exchange. These observations are in accord with the occurrence of kinetically-controlled quartz-water exchange, compared to local equilibrium exchange for calcite. Rate constants, calculated at 400 °C for experimental recrystallization exchange between calcite- and quartz-water from the equations in Table 1 of Cole and Ohmoto (1986), differ by an order of magnitude of ca. 1.5 and qualitatively agree with this interpretation. The higher $\delta^{18}O$ value for the mylonitic quartzite compared to the quartz of the mylonitic Lower Dolomite marble is explained by the far higher modal quartz in the quartzite.

The oxygen isotopic compositions of the dolomites indicate that they have not undergone exchange with the infiltrating fluids despite the clearly shown textural change related tectonism recognised in the rocks. This disparity between texture and isotopic changes is particularly marked in the mylonitic Lower Dolomite where the dolomite retains a high $\delta^{18}O$ value of 30.6‰ (Table 2). A precise comparison of the rate constants for calcite- and dolomite-water exchange as given in Table 1 of Cole and Ohmoto is not feasible because the authors' data for calcite is derived from experiments using pure water, whereas for dolomite they are obtained from experiments in which ammonium chloride was added to enhance exchange rates. A datum at 500 °C from the original dolomite-water partial exchange experiments of Northrop and Clayton (1966) in which ammonium carbonate was added to stabilize dolomite, but not to enhance exchange rates, yields a rate constant $\log r = -7.4$ close to that ($\log r = -7.6$) of quartz-water at the same temperature when recalculated using the equations of Cole and Ohmoto (1986). This suggests that dolomite exchanges at about the same rate as quartz. The absence of any indication of dolomite-fluid exchange in the Lower Dolomite sample is therefore surprising, even for the dominance of modal dolomite in the rock. Sample #9.4, an Upper Marble at the mylonite contact has almost equal amounts of dolomite and calcite but its analysis gives $\delta^{18}O$ ~20‰ for calcite and 31‰ for dolomite.

The failure of dolomite to exchange with the infiltrating fluid in the mylonite contact zone cannot therefore be simply explained by experimentally-derived rate constants. Other rheological factors are involved and two possibilities can be suggested. These are: (1) the dolomite was recrystallized prior to fluid infiltration and (2) the textural transformation of dolomite occurred during fluid infiltration, but did not involve isotopic exchange with the fluid. The former implies that thrust movement was initiated prior to the infiltration of significant amounts of fluid and by the time the fluids in-

filtrated, dolomite had effectively recrystallized. The latter indicates that potential mechanisms such as diffusional creep (Rutter and Brodie 1995) exist, which could allow a textural change in the dolomite to occur during fluid infiltration without recrystallization. On the basis of the present data, it is not possible to distinguish between these two models, but either case suggests that calcite recrystallization played a major role in the rheology of the shear zone movement with the aqueous fluid acting as the 'lubricant'.

Temperature distribution during thrusting

The temperature history for the rocks in the Panormos Bay area includes eclogite- and greenschist-facies metamorphism at ~450–500 °C in the Upper Marble and low grade metamorphism in the Lower Dolomite, accompanied by thermal resetting during and after the thrusting event. It is assumed for temperature analysis that the shape and values of the histograms presented in Fig. 6 reflect this history. The main petrological process that regulated the temperature measurement was the change in the Mg-content of calcite coexisting with dolomite. In the Panormos Bay sequences, thermometric resetting took place at temperatures below the diffusional closure of the calcite–dolomite system and therefore was governed by the recrystallization of calcite. Dolomite–calcite Mg-solvus temperatures therefore reflect the relative timing of calcite recrystallization, and given the connection between the recrystallization and the fluid infiltration, the relative timing and temperatures of fluid movement into the shear zone.

A progressive increase in temperatures with proximity to the contact was noted in the Lower Dolomite (Fig. 6a), with peak distributions at ~300 °C for #199 (−90 m); 340 °C for #200 (−50 m) and 370 °C for #212 (−40 m). This trend is consistent with the heating of the Lower Dolomite footwall by a hotter overlying plate. The $\delta^{18}O$ value for sample #199 is within the unaltered metamorphic marble range (Fig. 4), which suggests that its calcite did not undergo any recrystallization. Thus, it is possible that the 300 °C peak temperature distribution in the sample represents the low-grade metamorphism in the Lower Dolomite prior to thrusting. The peak temperatures ~360–420 °C observed in four Upper Marble samples (Fig. 6c) are too low to represent greenschist-facies conditions and therefore are interpreted to represent re-equilibration during cooling and thrusting. Two of these samples (#1, 10.3) show pronounced skewed distributions of temperatures down to 300 °C. This suggests a process of continuous resetting of the temperature during cooling and recrystallization. The final temperature of equilibration in the Upper Marble is probably ~300 °C, judging by the temperature distributions observed in samples # 10.4 and 206 with strain-free neo-formed calcite. The temperature distributions in these samples are considered to represent recrystallisation that terminated the ductile tectonic movement.

The apparently bimodal distributions of temperatures in samples from the mylonite zone (Fig. 6b) are less clear. The particularly well-defined temperature distribution for the Upper Marble (e.g. #9.4 with peaks at ~370–420 °C) could represent the re-equilibration event. The peak at 300 °C in the sample correspondingly represents the post-deformation recrystallization event already noted in samples #10.4 and 206. For the less well defined bimodal temperature distribution in the mylonite zone Lower Dolomite sample #9-3, the higher temperatures of ~400 °C may represent heating and recrystallization induced by the hotter upper plate. The lower temperature peak at ~300 °C indicates the late recrystallization event. The dolomite-calcite solvus exchange accompanying the fluid-enhanced calcite recrystallization gives temperatures that appear to broadly reflect the temperature history of both units during the thrusting event. It implies a heating of the Lower Dolomite from initial temperatures of ~300 °C, cooling of the Upper Marble from the greenschist-facies conditions of 450–500 °C to ~360–420 °C and continued cooling with a strain-free recrystallization at ~300 °C apparently terminating the thrusting process.

Conclusions

The aim of this study was to explore the thermal and rheological characteristics of a thrusting process related to the decompression of an alpine high P-T orogen. The study has demonstrated a unique stable isotope trend in the Panormos Bay marbles not yet observed in any other marble sequences of the ACM. The isotopic trend indicates that thrusting of marbles and schists of the Cycladic Blueschist Unit unto a lower grade dolomitic marble unit was associated with fluid-rock interaction that was focused along the tectonic contact. The measured depletions in the carbon and oxygen isotope signatures of calcite are consistent with the infiltration of a water-rich fluid $[X_C(=X_{CO_2}+X_{CH_4})<0.05]$ of metamorphic origin, whose carbon component was derived by the oxidation of organic matter. Small to moderate amounts of fluid (minimum W/R weight ratios <0.1–0.5) are indicated.

The results of the work are consistent with previous studies showing that fluid infiltration plays a critical role in shear-zone tectonic movement. An important aspect of the isotope results is that the fluid-rock interaction is mineralogically selective, only affecting calcite in the marbles. Even in the mylonite zone, dolomite coexisting with calcite does not show any significant isotopic shifts, despite having undergone textural change. Mylonitic quartz seems to undergo partial interaction with the infiltrating fluid. These differences can in part be attributed to kinetic factors; the slower rates of recrystallization and isotopic exchange of quartz and dolomite relative to calcite. These kinetic factors, however do not fully explain the apparent inertness of dolomite to water-rock isotopic exchange. It is attributed either to early

recrystallization of the dolomite before fluids were drawn into the tectonic process, or to a mechanism of dolomite textural change that does not involve solution-precipitation fluid-rock exchange. Fluid-induced calcite recrystallization is thus inferred to have played an important role in the rheology of the shear zone movement. It is proposed that the calcite-rich marble of the upper plate effectively glided over the less plastic dolomitic lower plate with the infiltrating fluid acting as a lubricant to the process.

Calcite recrystallization during the fluid infiltration resulted in dolomite-calcite solvus thermometry histograms that represent the temperature history during thrusting. Heating of the dolomitic marble lower plate to 350–400 °C from an initial temperature of 300 °C is inferred. Correspondingly, the hanging-wall calcite marble in the region of the tectonic contact shows a cooling from greenschist-facies conditions of 450–500 °C to 360–420 °C. Fluid infiltration to lower temperatures of ~300 °C is indicated in samples showing evidence of strain-free calcite recrystallization. Fluid infiltration in the shear zone was thus a prolonged process, though the thermometric and isotopic data do not explain if it was continuous, occurred in pulses or was spatially compartmented.

The extent of the thermometric resetting in the upper plate indicates that the thrusting probably resulted in a significant amount of conductive cooling in the plate. The relatively low calculated water/rock ratios do not suggest that convective cooling by advecting fluids was important. However, since thermometric resetting also reflects the timing of fluid infiltration, which shows considerable variation (as illustrated by the Upper Marble samples located within 25 m of the tectonic contact), the results are not appropriate for interpretation in terms of time-dependent heat-conduction models (e.g. England and Molnar 1993). The temperature range 350–420 °C obtained for samples near to the contact is close to the mean temperature 375–400 °C between an initial (pre-thrusting) upper plate temperature (450–500 °C, greenschist-facies conditions) and an initial lower plate temperature (300 °C, the low grade metamorphism in the Lower Dolomite). Thus, the thermometric results correspond to a simple model of conductive heat transfer that requires a final equilibration temperature equivalent to the mean of the initial temperature differences between the two plates.

The results of this study strongly support the observations of Avigad and Garfunkel (1989, 1995) and Avigad et al. (1997) that thrusting occurred during the decompression of the ACM. The absolute age constraints on timing of the thrusting are not known though the presence of greenschist-facies silicate lenses in the Upper Marble and the possibility that the infiltrating fluids were greenschist fluids imply that thrusting was relatively late in the orogenic history, and was either synchronous with or post-dated the greenschist-facies metamorphism. The Lower Dolomite Unit was shown to be a low temperature metamorphic unit prior to thrusting in accordance with the work of Avigad and Garfunkel (1989). In the wider context of the tectonic movement related to the decompression of the Alpine orogen, it is surmised that several rheological and thermal controls observed in the thrusting at Panormos Bay are generally applicable. These are: (1) fluid-induced recrystallization at low water/rock ratios was probably an important rheological control of thrusting, (2) the infiltrating fluids were locally derived and do not require long-range transport and (3) conductive heat transfer between the foot- and hanging-walls rocks may contribute to cooling at the base of the thrust unit.

Finally, this study reveals the relatively low $\delta^{18}O$ values in late quartz veins that cut the Panormos Bay sequence (Fig. 2; Table 2). These veins probably formed by downward movement of meteoric water from the surface along a steep normal fault system that developed during the later extensional tectonism in the ACM. For the vein samples, a formation temperature of 200 °C would give oxygen isotopic compositions of ground waters similar to present-day rainwater in the southern European region. At a normal continental geothermal gradient of ~25°/km, such a temperature would imply deep meteoric water penetration to depths of 8 km. A more speculative proposal is that the veins formed closer to the surface at lower temperatures (e.g. 100 °C). Quartz- water fractionation at 100 °C is ~20‰. (Matsuhisa et al. 1979; Matthews and Beckinsale 1979) and gives water $\delta^{18}O$ values in the range −15 to −12‰, significantly lower than found in present-day rainwaters. However, if an elevated mountain topography existed then lower isotopic compositions could be obtained for rainwaters, as are observed in the Alps today (Rozanski et al. 1993).

Acknowledgements The authors are indebted to Dr Rainer Abart for his extremely perceptive comments, which have lead to considerable improvement and revision of the manuscript. Dr. Avner Ayalon, Avi Bosaglou-Yoresh and Ran Yogev are thanked for help with the analyses. Dr. Benita Putlitz kindly performed the laser fluorination analyses. Discussions with Dr. Judy Baker on the modelling and presentation of the data are very much appreciated. The research was supported by a grant from the Israeli Ministry of Sciences in cooperation with the European Economic Community. Construction of the laser probe fluorination system was in part supported by a grant from the Israel Science Foundation funded by the Israel Academy of Sciences and Humanities.

References

Abart R, Sperb R (1997) Grain-scale stable isotope disequilibrium during fluid-rock interaction. 1: Series approximations for advective-dispersive transport and first-order kinetic mineral-fluid exchange. Am J Sci 297: 679–706

Altherr R, Henjes-Kunst FJ, Wendt I, Lenz H, Wagner GA, Keller J, Harre W, Hohndorf A (1982) A Late Oligocene/Early Miocene high temperature belt in the Attic- Cycladic crystalline complex (SE Pelagonian, Greece). Geol Jahrbuch E23: 97–164

Altherr R, Henjes-Kunst FJ, Matthews A, Friedrichsen H, Hensen BT (1988) O-Sr isotopic variations in Miocene granitoids from the Aegean: evidence for an origin by combined assimilation and fractional crystallisation. Contrib Mineral Petrol 100: 528–541

Avigad D (1993) Tectonic juxtaposition of blueschists and greenschists on Sifnos island (Aegean Sea): implications for the structure of the Cycladic blueschist belt. J Struct Geol 15: 1459–1469

Avigad D, Garfunkel Z (1989) Low-angle faults above and below a blueschist belt-Tinos island, Cyclades (abstract). Terra Nova [Suppl] 1: 182–187

Avigad D, Garfunkel Z (1991) Uplift and exhumation of high-pressure metamorphic terrains: the example of the Cycladic blueschist belt. Tectonophysics 188: 357–372

Avigad D, Garfunkel Z (1995) Back-arc extension and the exhumation of Mediterranean eclogites. Terra Abstr 7: 121

Avigad D, Matthews A, Evans BW, Garfunkel Z (1992) Cooling during the exhumation of a blueschist terrane: Sifnos (Cyclades), Greece. Eur J Mineral 4: 619–634

Avigad D, Garfunkel Z, Jolivet L, Azanon JM (1997) Back arc extension and denudation of Mediterranean eclogites. Tectonics 16: 924–941

Baker J, Matthews A (1994) Textural and isotopic development of marble assemblages during Barrovian-style M2 metamorphic event, Naxos, Greece. Contrib Mineral Petrol 116: 130–144

Baker J, Matthews A (1995) The stable isotope evolution of a metamorphic complex, Naxos, Greece. Contrib Mineral Petrol 120: 391–403

Baker J, Spiegelman M (1995) Modeling of an infiltration driven geochemical front. Earth Planet Sci Lett 136: 87–96

Baker J, Bickle MJ, Buick IS, Holland TJB, Matthews A (1989) Isotopic and petrological evidence for the infiltration of a water-rich fluid during the Miocene M2 metamorphism on Naxos, Greece. Geochim Cosmochim Acta 53: 2037–2050

Banks DA, Davies GR, Yardley BWD, McCaig AM, Grant NT (1991) The chemistry of brines from an alpine thrust system in the Central Pyrenees: an application of fluid inclusion analysis to the study of fluid behaviour in orogenesis. Geochim Cosmochim Acta 55: 1021–1030

Baumgartner L, Rumble III D (1988) Transport of stable isotopes: I: development of a kinetic continuum theory for stable isotope transport. Contrib Mineral Petrol 98: 417–430

Beach A (1976) The interrelations of fluid transport and heat flow in Early Proterozoic shear zones in the Lewisian complex. Philos Trans R Soc Lond A 280: 569–604

Beach A, Fyfe WS (1972) Fluid transport and shear zones at Scourie, Sutherland. Evidence for overthrusting. Contrib Mineral Petrol 32: 175–180

Bickle M, Baker J (1990) Advective-diffusive transport of isotopic fronts: an example from Naxos, Greece. Earth Planet Sci Lett 97: 78–93

Bickle M, McKenzie D (1987) The transport of heat and matter by fluids during metamorphism. Contrib Mineral Petrol 95: 382–392

Bottinga Y (1969) Calculated fractionation factors for carbon and hydrogen isotope exchange in the system calcite-CO2-graphite-methane-hydrogen and water vapor. Geochim Cosmochim Acta 33: 49–64

Bröcker M (1990) Blueschist-to-greenschist transition in metabasites from Tinos Island, Cyclades, Greece: compositional control or fluid infiltration. Lithos 25: 25–39

Bröcker M, Kreuzer H, Matthews A, Okrusch M (1993) $^{40}Ar/^{39}Ar$ and oxygen isotope studies of polymetamorphism from Tinos island, Cycladic blueschist belt, Greece. J Metamorph Geol 11: 223–240

Buick IS (1991) The late alpine evolution of an extensional shear zone, Naxos, Greece. J Geol Soc Lond 148: 93–103

Burkhard M, Kerrich R (1988) Fluid regimes in the deformation of the Helvetic nappes, Switzerland, as inferred from stable isotope data. Contrib Mineral Petrol 99: 416–429

Burkhard M, Kerrich R, Maas R, Fyfe WS (1992) Stable and Sr isotope evidence for fluid advection during thrusting of the Glarus nappe (Swiss Alps). Contrib Mineral Petrol 112: 293–311

Cartwright I, Valley JW, Hazelwood AM (1993) Resetting of oxybarometers and oxygen isotope ratios in granulite facies orthogneisses during cooling and shearing. Contrib Mineral Petrol 113: 208–225

Chacko T, Mayeda TK, Clayton RN, Goldsmith JR (1991) Oxygen and carbon isotope fractionations between CO_2 and calcite. Geochim Cosmochim Acta 55: 2867–2882

Clayton RN, Mayeda TK (1963) The use of bromine pentafluoride in the extraction of oxygen from oxides and silicates for isotopic analysis. Geochim Cosmochim Acta 27: 43–52

Cole DR, Ohmoto H (1986) Kinetics of isotope exchange at elevated temperatures and pressures. In: Valley JW, Taylor HP Jr, O'Neil JR (eds) Stable isotopes in high temperature geological processes. Mineralog Soc Am Rev Mineral 16: 41–90

Crespo-Blanc AC, Masson H, Sharp Z, Cosca M, Hunziker M (1995) A stable and $^{40}Ar/^{39}Ar$ isotope study of a major thrust in the Helvetic nappes (Swiss Alps): evidence for fluid flow and constraints on nappe kinematics. Geol Soc Am Bull 107: 1129–1144

Connolly JAD, Cesare B (1993) C—O—H—S fluid composition and oxygen fugacity in graphitic metapelites. J Metamorph Geol 11: 379–388

Crittenden MDJ, Coney PJ Davis GH (1980) Cordilleran metamorphic core complexes. Geol Soc Am Memoir 153: 490

Durr S, Altherr R, Keller J, Okrusch M, Seidel E (1978) The median Aegean crystalline belt: stratigraphy, structure, metamorphism, magmatism. In: Cloos H, Roedder D, Schmidt K (eds) Alps, Appenines, Hellenides. Schweiz Barts'che, Stuttgart, pp 455–476

England PC, Molnar P (1993) The interpretation of inverted metamorphic isograds using simple physical calculations. Tectonics 12: 145–157

England PC, Thompson AB (1984) Pressure-temperature-time paths of regional metamorphism. 1. Heat transfer during the evolution of regions of thickened crust. J Petrol 25: 894–928

Eppel H, Abart R (1997) Grain-scale stable isotope disequilibrium during fluid-rock interaction. 2: an example from the Penninic-Austroalpine tectonic contact in Eastern Switzerland. Am J Sci 297: 707–728

Essene EJ (1985) Solid solutions and solvi among metamorphic carbonate with applications to geological thermometry. In: Reeder RJ (ed) Carbonates: mineralogy and chemistry. Mineral Soc Am Rev Mineral 11: 77–96

Etheridge MA, Wall VJ, Fox SF (1984) High fluid pressures during regional metamorphism and deformation: implications for mass transport and deformation mechanisms. J Geophys Res 89: 4344–4388

Fourcade S, Marquer D, Javoy M (1989) $^{18}O/^{16}O$ variations and fluid circulation in a deep shear zone: the case of the Alpine ultramylonites from the Aar Massif (Central Alps, Switzerland). Chem Geol 77: 119–132

Fricke HC, Wickham SM, O'Neil JR (1992) Oxygen and hydrogen isotope evidence for meteoric water infiltration during mylonitization and uplift in the Ruby Mountains-East Humboldt Range core complex, Nevada. Contrib Mineral Petrol 111: 203–221

Fyfe WS, Kerrich R (1985) Fluids and thrusting. Chem Geol 49: 353–362

Ganor J, Matthews A, Paldor N (1989) Constraints on effective diffusivity during oxygen isotope exchange at a marble – schist contact, Sifnos (Cyclades) Greece. Earth Planet Sci Lett 94: 208–216

Ganor J, Matthews A, Paldor N (1991) Diffusional isotopic exchange across an interlayered marble-schist sequence with an application to Tinos, Cyclades, Greece. J Geophys Res 96: 18073–18080

Ganor J, Matthews A, Schliestedt M (1994) Post metamorphic low $\delta^{13}C$ calcite veins in the Cycladic complex (Greece) and their implications for modeling fluid infiltration processes using carbon isotope compositions. Eur J Mineral 6: 365–379

Ganor J, Matthews A, Schliestedt M (1996) Oxygen isotope heterogeneities of metamorphic rocks: an original tectonostratigraphic signature, or an imprint of exotic fluids? A case study of Sifnos and Tinos islands (Greece). Eur J Mineral 8: 128–138

Gat JR (1996) Oxygen and hydrogen isotopes in the hydrologic cycle. Ann Rev Earth Planet Sci 24: 225–262
Gautier P, Brun JP (1994) Crustal-scale geometry and kinematics of late-orogenic extension in the central Aegean (Cyclades and Evvia Island). Tectonophysics 238: 399–424
Gautier P, Brun JP, Jolivet L (1993) Structure and kinematics of upper Cenozoic extensional detachment on Naxos and Paros (Cyclades islands, Greece). Tectonics 12: 1180–1194
Goldsmith JR, Newton RC (1969) P-T-X relations in the system $CaCO_3$-$MgCO_3$ at high temperatures and pressures. Am J Sci 267A: 160–190
Grant NT, Banks DA, McCaig AM, Yardley BWD (1990) Chemistry, source, and behaviour of fluids involved in alpine thrusting of the Central Pyrenees. J Geophys Res 95: 9123–9131
Hubbert MK, Rubey WW (1959) Role of fluid pressure in the mechanics of overthrust faulting. Geol Soc Am Bull 70: 115–166
Katzir Y, Matthews A, Garfunkel Z, Schliestedt M, Avigad D (1996) Tectono-metamorphic evolution of a dismembered metamorphosed ophiolite; Tinos island (Cyclades, Greece). Geol Mag 133: 237–254
Kerrich R, La Tour TE, Willmore L (1984) Fluid participation in deep fault zones: evidence from geological, geochemical, and $^{18}O/^{16}O$ relations. J Geophys Res 89: 4331–4343
Kolodny Y, Epstein S (1976) Stable Isotope geochemistry of deep sea cherts. Geochim Cosmochim Acta 40: 1195–1209
Kreulen R (1988) High integrated fluid/rock ratios during metamorphism at Naxos: evidence from carbon isotopes and fluid inclusions. Contrib Mineral Petrol 98: 28–32
Lee J, Lister GS (1992) Late Miocene ductile extension and detachment faulting: Mykonos, Greece. Geology 20: 121–124
Lieberman JE, Rice JM (1986) Petrology of marble and peridotite in the Seiad Ultramafic complex, Northern California, USA. J Metamorph Geol 4: 179–199
Lister GS, Banga G, Feenstra A (1984) Metamorphic core complexes of the Cordilleran type in the Cyclades. Geology 12: 221–225
Matsuhisa Y, Goldsmith JR, Clayton RN (1979) Oxygen isotope fractionation in the system quartz-albite-anorthite-water. Geochim Cosmochim Acta 43: 1131–1140
Matthews A, Beckinsale RD (1979) Oxygen isotope equilibration systematics between quartz and water. Am Mineral 64: 232–240
Matthews A, Katz A (1977) Oxygen isotope fractionation during the dolomitization of calcium carbonate. Geochim Cosmochim Acta 41: 1431–1438
Matthews A, Schliestedt M (1984) Evolution of the blueschist and greenschist facies rocks of Sifnos, Cyclades, Greece. A stable isotope study of subduction related metamorphism. Contrib Mineral Petrol 88: 150–163
McCaig AM (1988) Deep circulation in fault zones. Geology 16: 867–870
McCaig AM, Wickham SM, Taylor HPJ (1990) Deep fluid circulation in Alpine shear zones, Pyrenees, France: field and oxygen isotope studies. Contrib Mineral Petrol 106: 41–60
McCaig AM, Wayne DW, Marshall JD, Banks D, Henderson I (1995) Isotopic and fluid inclusion studies of fluid movement along the Gavarnie thrust, Central Pyrenees: reaction fronts in carbonate mylonites. Am J Sci 295: 309–343
McCrea JM (1950) On the isotopic chemistry of carbonates and paleotemperature scale. J Chem Phys 18: 849–857
Melidonis NG (1980) The geological structure and mineral deposits of Tinos island (Cyclades, Greece). IGME Athens, The Geology of Greece 13: 1–80
Morrison J (1994) Downward circulation of meteoric water into the lower plate of the Whipple Mountains metamorphic core complex, California. J Metamorph Geol 12: 827–840
Morrison J, Lawford Anderson J (1998) Footwall refrigeration along a detachment fault: implications for the thermal evolution of a core complex. Science 279: 63–66
Northrop DA, Clayton RN (1966) Oxygen isotope fractionation in systems involving dolomite. J Geol 74: 174–196
Okrusch M, Bröcker M (1990) Eclogites associated with high-grade blueschists in the Cycladic archipelago, Greece: a review. Eur J Mineral 2: 451–478
Oliver NHS, Cartwright I, Wall VJ, Golding SD (1993) The stable isotope signature of large-scale fracture hosted metamorphic fluid pathways, Mary Kathleen, Australia. J Metamorph Geol 11: 705–720
O'Neil JR, Clayton RN, Mayeda TK (1969) Oxygen isotope fractionation in divalent metal carbonates. J Chem Phys 51: 5547–5558
Peters MT, Wickham SM (1994) Petrology of amphibolite facies marbles from the eastern Humboldt Ranges, Nevada, USA: evidence for high temperature, retrograde hydrous volatile fluxes at mid-crustal levels. J Petrol 35: 205–238
Platt JB (1987) The uplift of high-pressure-low-temperature metamorphic rocks. Philos Trans R Soc Lond A 321: 87–103
Platt JB (1993) Exhumation of high-pressure metamorphic rocks: a review of concepts and processes. Terra Nova 5: 119–133
Reynolds SJ, Lister GS (1987) Structural aspects of fluid-rock interactions in detachment zones. Geology 15: 362–366
Ridley JR (1984) Listric normal faulting and the reconstruction of the synmetamorphic pile of the Cyclades. In: Dixon J, Robertson AHF (eds) The geological evolution of the Eastern Mediterranean. Geol Soc Lond Spec Publ 17: 755–762
Rozanski K, Araguas-Araguas L, Gongiantini R (1993) Isotopic patterns in modern global precipitation. In: Swart PK, Lohmann KG, McKenzie JA (eds) Climate patterns in continental isotopic records. Am Geophys Union Geophys Monogr 78: 1–36
Rutter EH, Brodie KH (1995) Mechanistic interactions between deformation and metamorphism. Geol J 30: 227–240
Rye DM, Bradbury HJ (1988) Fluid flow in the crust: an example from a Pyrenean thrust ramp. Am J Sci 288: 197–235
Rye RO, Schuiling RD, Rye DM, Jansen JBH (1976) Carbon, hydrogen, and oxygen isotope studies of the regional metamorphic complex at Naxos, Greece. Geochim Cosmochim Acta 40: 1031–1049
Schliestedt M (1986) Eclogite–blueschist relationships evident by mineral equilibria in the high-pressure metabasic rocks of Sifnos (Cycladic islands). J Petrol 27: 1437–1459
Schliestedt M, Matthews A (1987) Transformation of blueschist to greenschist facies rocks as a consequence of fluid infiltration. Contrib Mineral Petrol 97: 237–250
Schliestedt M, Altherr R, Matthews A (1987) Evolution of the Cyclades crystalline complex: petrology, isotope geochemistry and geochronology. In: Helgeson HC (ed) Chemical transport in metasomatic processes. D. Reidel, NATO ASI Ser 218C: 389–428
Schliestedt M, Bartsch V, Carl M, Matthews A, Henjes-Kunst F (1994) The P-T path of Greenschist-facies rocks from the island of Kithnos (Cyclades, Greece). Chem Erde 54: 281–296
Sibson RH, McMoore J, Rankin AH (1975) Seismic pumping – a hydrothermal fluid transport mechanism. J Geol Soc Lond 131: 653–659
Stolz J, Engi M, Rickli M (1997) Tectonometamorphic evolution of SE Tinos, Cyclades, Greece. Schweiz Mineral Petrol Mitt 77: 209–232
Taylor HP Jr (1977) Water/rock interactions and the origin of H_2O in granitic batholiths. J Geol Soc Lond 133: 509–558
Thompson AB, Ridley JR (1987) Pressure-time-temperature (P-T-t) histories of orogenic belts. In: Oxburgh ER, Yardley BWD, England PC (eds) Tectonic settings of regional metamorphism. Philos Trans R Soc Lond A 32: 27–45
Wijbrans JR, Schliestedt M, York D (1990) Single grain argon laser probe dating of phengites from the blueschist to greenschist transition on Sifnos (Cyclades, Greece). Contrib Mineral Petrol 104: 582–593